Author's Accepted Manuscript

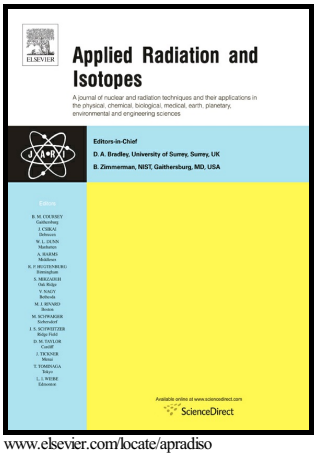

www.elsevier.com/locate/apradiso

Evaluation of dosimetric properties of shielding disk used in intraoperative electron radiotherapy: A Monte Carlo study

Mostafa Robatjazi, Hamid Reza Baghani, Seied Rabi Mahdavic, Giuseppe Felici

PII: S0969-8043(17)31127-2
DOI: https://doi.org/10.1016/j.apradiso.2018.04.037
Reference: ARI8348

To appear in: *Applied Radiation and Isotopes*

Received date: 23 September 2017
Revised date: 26 February 2018
Accepted date: 30 April 2018

Cite this article as: Mostafa Robatjazi, Hamid Reza Baghani, Seied Rabi Mahdavic and Giuseppe Felici, Evaluation of dosimetric properties of shielding disk used in intraoperative electron radiotherapy: A Monte Carlo study, *Applied Radiation and Isotopes,* https://doi.org/10.1016/j.apradiso.2018.04.037

This is a PDF file of an unedited manuscript that has been accepted for publication. As a service to our customers we are providing this early version of the manuscript. The manuscript will undergo copyediting, typesetting, and review of the resulting galley proof before it is published in its final citable form. Please note that during the production process errors may be discovered which could affect the content, and all legal disclaimers that apply to the journal pertain.

ACCEPTED MANUSCRIPT

Evaluation of dosimetric properties of shielding disk used in intraoperative electron radiotherapy: A Monte Carlo study

Mostafa Robatjazi[a,b], Hamid Reza Baghani[c]*, Seied Rabi Mahdavic[d], Giuseppe Felici[e]

[a]Department of Medical Physics and Radiological Sciences, Sabzevar University of Medical Sciences, Tohid Shahr St 9613873136, Sabzevar, Iran

[b]Vasei Radiotherapy & Oncology Center, Vasei hospital, Sabzevar University of Medical Sciences, Tohid Shahr St 9613873136, Sabzevar, Iran

[c]Physic Department, Hakim Sabzevari University, Tohid Shahr St 961797647, Sabzevar, Iran

[d]Department of Medical Physics, Iran University of Medical Sciences, Hemmat Exp. Way 14496141525, Tehran, Iran

[e]Department of SIT R&D, dell' Industria1, Aprilia, Italy

*Corresponding author: Hamid Reza Baghani. E-mail address: Hamidreza.baghani@gmail.com

Accepted manuscript

Abstract

A shielding disk is used for IOERT procedures to absorb radiation behind the target and protect underlying healthy tissues. Setup variation of shielding disk

ACCEPTED MANUSCRIPT

can affect the corresponding in-vivo dose distribution. In this study, the changes of dosimetric parameters due to the disk setup variations is evaluated using EGSnrc Monte Carlo (MC) code. The results can help treatment team to decide about the level of accuracy in the setup procedure and delivered dose to the target volume during IOERT.

Keywords: IOERT; breast cancer; shielding disk; Monte Carlo simulation

Accepted manuscript

1. Introduction

Intraoperative radiation therapy (IORT) refers to delivery of a single high dose of irradiation directly to the tumor bed after resection. Intraoperative electron

ACCEPTED MANUSCRIPT

radiotherapy (IOERT) is an IORT technique in which electron beams with different nominal energies are used for irradiation of microscopic residual after surgery (Intra et al. 2006, Robatjazi et al. 2015). Direct visualization of the target, administration of homogenous dose to the target, and the possibility of protecting normal tissues by moving them away from the beam path are the most important advantages of IOERT.

Employing a shielding disk, which is positioned under the target volume, for protecting the normal tissues such as pectoral muscle, lung, and heart is one of the advantages of IOERT in the breast cancer treatment (Ciocca et al. 2012, López-Tarjuelo et al. 2014). To have a sufficient attenuation of the electron beam, it is important to select an effective shield composition to minimize both backscatter and transmitted radiation. Various compositions have been introduced by different manufacturers for these disks. A common characteristic of these disks is double-layer format; a high atomic number (Z) layer with the ability to absorb the electron beam to prevent penetration to deeper tissues and a low-Z layer on top of the former to minimize the backscattered electrons from the lower layer. (Catalano et al. 2007, Martignano et al. 2007, Oshima et al. 2009).

Backscatter effect of these shields can change the dose distribution inside the target. In some cases, a significant increase in delivered dose to the distal end of target volume has been observed. There are many studies about optimal

Accepted manuscript

ACCEPTED MANUSCRIPT

thickness and composition of shielding disk layers. Martignano et al. evaluated the application of a single high-Z layer, single low-Z layer, and double-layers as a shielding disk for IOERT. They concluded that attenuation and backscatter factor (BSF) of double layer disks are better than single layer ones (Martignano et al. 2007). Oshima et al. studied the selection of the optimum thickness of polymethyl methacrylate (PMMA) as a low-Z layer and Copper (Cu) as a high-Z layer for design and construction of the shielding disk, using EGS4 MC code. The optimum thickness of mentioned layers was obtained as 0.71 cm for PMMA and 0.3 cm for Cu. They reported that maximum BSF of this configuration was about 1% (Oshima et al. 2009). Catalano et al. assessed the impact of various compositions of shielding disks on backscatter effect at different depths along the central axis of the electron beam through Fluka MC code (Catalano et al. 2007). They concluded that the application of high Z material (Pb or Cu) reduces the transmitted dose down to 7% in 7 MeV electron beam energy. Furthermore, their study showed that application of double-layer disks can reduce the BSF. Russo et al. evaluated the effect of shielding disk misalignments (4 mm Al + 2 mm Pb) on target dose distribution using GEANT4 MC code for a NOVAC7 machine (Russo et al. 2012). They reported that the BSF of mentioned disk configuration is about 10% and mean shielding factor (SF) is about 97%. Furthermore, the conclusion of their study showed that the lateral translation of disk does not significantly influence the dose

Accepted manuscript

ACCEPTED MANUSCRIPT

distribution inside the target, and homogeneity of target dose was acceptable with disk rotations up to 10°.

Misalignments of shielding disk including positioning and angulation errors can have a considerable effect on dose uniformity inside target area and received dose to the underlying normal tissues. Severgnini et al. evaluated the shielding disk alignment in the breast IOERT using EBT3 films, however, it was not an appropriate method to evaluate the position of shielding disk on site and its effect on the dose distribution in the target, because it is time-consuming to scan and read-out the film (Severgnini et al. 2014). Furthermore, dosimetric uncertainties of film dosimetry can be larger than the magnitude of the backscatter dose due to the presence of shielding disks (Baghani et al. 2015, Robatjazi et al. 2015, Yekta et al. 2016). An alternative method is intraoperative imaging using a C-arm system. This method is reliable, online and can show any setup error of shielding disk and/or employed applicator.

In this study, we have evaluated the misalignment effects of shielding disk on dose distribution inside the target and surrounding normal tissues through EGSnrc MC Simulation. MC simulation is one of the applicable methods for evaluating the dose distribution at complicated geometries and regions where dose measurement is difficult. Furthermore, MC simulation is not subject to the problems of film and ionometric dosimetry methods and can be used to design material without fabrication and measurement requirements.

Accepted manuscript

ACCEPTED MANUSCRIPT

2. Material and Methods

2.1. Mobile dedicated IOERT machine

LIAC 12 (Sordina IORT Technologies S.p.A, Vicenza, Italy, SN 0034) is a dedicated IOERT machine that can produce electron beam energies of 6, 8, 10, 12 MeV. Dose rate varies from 10 to 25 Gy per minute and the pulse repetition frequency ranges from 1 to 60 Hz (depending on beam energy). The length of accelerating structure, including 19 self-focusing cavities, is equal to 925 mm. The 0.82 mm thick Al scattering foil reduces the probability of neutron production at high energies (Gunderson et al. 2011, Baghani et al. 2015, Heidarloo et al. 2017). Employed applicators are composed of PMMA cylindrical tubes with the thickness of 5 mm. The diameter and base angle of these applicators range from 30 to 100 (30, 40, 50, 60, 70, 80, and 100) mm and 0 to 45(0, 15, 30, and 45) degrees, respectively. Length of these applicators is 600 mm, providing a distance between scattering foil and applicator end (SSD) of 713 mm (Gunderson et al. 2011, Heidarloo et al. 2017). A hard docking mechanism is applied to collimate electron beam in this machine (Gunderson et al. 2011).

Accepted manuscript

2.2. Shielding disk

A dedicated shielding disk can be used to absorb radiations behind the target and protect underlying healthy tissues. The disk is particularly recommended for breast IOERT for healthy tissue protection. Shielding disk must be

ACCEPTED MANUSCRIPT

positioned by the surgeon inside the human body, between the glandular tissue and the pectoral muscle surface. The disk can be sterilized with water vapor up to 134°C. They are available in diameters of 40, 50, 60, 70, 80, and 90 mm. The disks are composed of a 3 mm layer of polytetrafluoroethylene (PTFE) as a low-Z layer and a 3 mm stainless steel as a high-Z layer. During the treatment delivery, the disk is placed in such a way that the low-Z layer (PTFE) is faced with the incident electron beam. The choice of these materials provides biocompatibility, secure disk cleaning and sterilizing procedures and effective attenuation of the intra-operative electron beam.

2.3. Monte Carlo simulation

2.3.1. LIAC head simulation

Machine head was modeled using the BEAMnrc MC code in this study (Rogers et al. 2002). The machine head data and materials employed in the MC simulation were provided by the manufacturer (Sordina, SpA, Italy). The EGSnrc SLAB module was used to model the exit window of the waveguide and scattering foil that are made of titanium and aluminum, respectively. To simulate the LIAC head structures and applicators, the FLATFILT module was used. The CHAMBER module was employed to monitor ion chambers modeling and the final exit window of the head, which is made of Mylar. The cross sections of all materials were taken from ICRU521 EGSnrc library. Some materials that are not included in this file were added to this library. For each

Accepted manuscript

ACCEPTED MANUSCRIPT

simulation process, the number of histories was set to 2-3×10E8. Cut off energies for electron and photon (ECUT, PCUT) were 0.521 MeV and 0.01 MeV, respectively. The specification of electron source above the titanium window, for extraction of phase space files, was defined by ISOURC =19 module as a Gaussian distributed intensity profile. Full width of half maximum for source spatial distribution was chosen as 2 mm and the mean angular spread of electron beam was set to 0°. The energy distribution of electron beam at different energies was defined with 0.1 MeV increments. Scoring planes were defined at the bottom of the applicator. The output of BEAMnrc code is a phase-space file that contains information such as energy, charge, position, direction, angle, and weight of every particle that crosses a given scoring plane. These phase-space files were used as an input in other codes for calculation of dose distribution (Rogers et al. 2002, Robatjazi et al. 2016).

2.3.2. Monte Carlo validation

Before evaluating the dose distribution around the shielding disk, it was necessary to validate the MC simulated model of LIAC head. Therefore, percentage depth dose (PDD) and transverse dose profiles (TDP) for different electron energies of LIAC machine (6, 8, 10, 12 MeV) were measured inside a 3D scanning water phantom (MP3-XS, PTW, Freiburg, Germany) using Advanced-Markus ion chamber (PTW, Freiburg, Germany) and were compared with those obtained by MC calculations. It should be mentioned that all

Accepted manuscript

ACCEPTED MANUSCRIPT

measurements were performed for 100 mm diameter flat applicator (reference applicator).

The phase-space files for the reference applicator (diameter = 100 mm, SSD =713 mm), were used as an input in the DOSXYZnrc code for MC calculations (Ma et al.). To calculate the PDD and TDP, water phantom dimensions were assumed to be 30×30×15 cm^3 and voxel size was 2×2×2 mm^3. In order to evaluate the agreement between the PDDs and TDPs derived from MC simulation and experimental values obtained by ion chamber, gamma analysis was used as recommended by Low et al (Low et al. 1998). Dose difference and distance to agreement (DTA) criteria in calculations of the gamma index were set as 2% and 2 mm, respectively (Low and Dempsey 2003). Gamma index values between zero and one were considered as pass (agreement between obtained results), while values greater than one were considered as a fail (disagreement between the obtained results). It should be noted that the gamma index calculations were performed in DoseLab Pro (Mobius Medical Systems, LP, Houston, TX).

Accepted manuscript

2.3.3. Shielding disk simulation

The circular geometry of the shielding disk and evaluation of the dose distribution around the disk, in various angles and positions, needs a code to model these complicated geometries and score the dose values in arbitrary regions. Although it is possible to model the circular and cylindrical geometries

ACCEPTED MANUSCRIPT

in the DOSRZnrc code (Rogers et al. 2003), this code is not able to model the disk in angular position inside water phantom. One of the EGSnrc based codes that allow us to model the complicated geometries, source, and dose scoring inside any arbitrary region is EGSnrc C++ class library (Kawrakow 2005, Kawrakow et al. 2009). In this study, we used the EGSnrc C++ class library for calculation of the dose distribution around the shielding disk. To simulate both layers of the shielding disk that mentioned above, the egs_planes, egs_cylinders, and egs_ndgeometry libraries were used. The egs_ndgeometry library was used for simulation of the voxelized water phantom.

To simulate the disk in the water phantom, the egs_genvelope library was used. For this purpose, water phantom and disk were considered as "base geometry" and "inscribed geometry", respectively. The "egs_gtransformed" library was used to simulate the disk at any arbitrary depth and angle. Fig. 1 shows the simulated shielding disk inside the water phantom.

2.4. Dose distribution evaluation around the shielding disk

Based on our experience in breast IOERT procedures, almost all of the disk positions relative to applicator must be changed to be in correct setup. An effective method to control and correct the setup of the disk relative to the applicator during IOERT is visualization by C-arm imaging. Fig. 2 shows the C-arm image of an incorrect disk setup in breast IOERT.

Accepted manuscript

ACCEPTED MANUSCRIPT

To evaluate the dose distribution around the disk, disk surface was simulated at the depth of 90% dose (R90) for each nominal energy. Then, the PDD curves for all machine energies were calculated along the beam central axis in presence and absence of disk at the mentioned depth. The SF, BSF, and percentage of leakage dose (PLD) were the considered parameters for quantification of dose around the disk.

The SF is defined by the following equation (Eq. 1):

$$SF = \frac{D_{w/o} - D_w}{D_{w/o}} \times 100 \quad (1)$$

Where $D_{w/o}$ is the dose without disk, and D_w is the dose at the same position in presence of the disk.

The BSF is defined as the ratio of the dose value with and without the disk (as shown in Eq. 2):

$$BSF = \frac{D_w}{D_{w/o}} \times 100 \quad (2)$$

Where the D_w is dose value at the presence of disk and $D_{w/o}$ is dose value at the same depth in absence of the disk.

PLD is defined as the percentage of maximum leakage dose after the disk and is obtained according to the following equation (Eq. 3):

$$PLD = \frac{D_t}{D_{\max}} \times 100 \quad (3)$$

Accepted manuscript

ACCEPTED MANUSCRIPT

Where D_t is the dose value immediately after the shielding disk and D_{max} is the maximum dose (above the shielding disk) along the central axis.

Occurred errors during breast IOERT setups such as transverse displacement of the disk relative to applicator or placement of the disk at an angular position relative to the applicator, may affect the dose distribution inside the target and in some cases, can impair the shielding by the disk. To evaluate these effects, the dose distribution was calculated inside the target and underlying normal tissues for erroneous disk positions at different angles (0°, 5°, 10°, 20°, 30°) relative to the applicator. We also considered a condition that the disk was in the reversed state where the high-Z material of the disk was faced with the incident electron beam.

In this study, we also used differential-DVHs to evaluate the dose distributions, both in correct and incorrect disk setups. The DVH is a powerful tool to summarize and quantify the dose distribution inside the target and normal tissue in order to evaluate radiotherapy treatment planes. One of the most important benefits of DVH is providing an accurate assessment of dose uniformity inside the target.

To evaluate the dose uniformity inside the target area, the S-index was used. This parameter has been proposed by Yoon et al. Emphasis of the S-index and priority of this quantity relative to the standard homogeneity indexes, has been shown in their study (Yoon 2007).

Accepted manuscript

ACCEPTED MANUSCRIPT

2.5. Experimental measurement of BSF

To evaluate and verify the calculated BSFs, the BSF for each nominal energy was measured using the Advanced-Markus chamber inside the MP3-XS water phantom (PTW, Freiburg, Germany). For this purpose, the chamber was placed at the R90 depth of each nominal energy. At the first state, the chamber was located at the top surface of shielding disk (PTFE layer) in reverse position and irradiations were repeated three times. At the second state, just the disk was removed and irradiations were repeated under the same conditions. Finally, the BSF at different nominal energies was calculated by dividing the chamber reading in presence of disk to that of disk absence at the corresponding energy.

3. Results

3.1. MC validation

There was good agreement between calculated and measured data for both PDDs and TDPs. Corresponding gamma values for PDD and TDPs of the four beam energies was lower than one in more than 95% of studied depths and off-axis distances which quantitatively confirms the validity of the performed simulations.

The PDD parameters for each energy of LIAC electron beam, which was measured by Advanced-Markus chamber and MC simulation, are presented in Table 1.

3.2. Dosimetric parameters around shielding disk

Accepted manuscript

ACCEPTED MANUSCRIPT

In the first step of evaluating disk dosimetric parameters in the correct and reversed position, the PDD curves for different energies were calculated along the beam central axis, in presence and absence of shielding disk at the corresponding R90 depth of each energy. The simulated PDD for 12 MeV energy in presence and absence of shielding disk is shown in Fig. 3.

Incorrect configurations were simulated for all energies at 5°, 10°, 20°, and 30° rotation of shielding disk relative to the applicator. It should be mentioned that the central axis of the applicator was considered as the reference axis for disk rotation.

The MC simulated and experimental value of BSF for all nominal energies in the mentioned configurations are shown in Fig. 4. As depicted in this figure, the simulated values range from 1.03 to 1.11 and the experimental values range between 1.02 and 1.1 for all studied energies.

Fig. 5 shows the SF and corresponding PLD values for all energies. The SFs for 6 and 8 MeV beam energies were not considerable in the correct setup. By increasing the degree of disk rotation and beam energy, the SF decreases and, as expected, PLD would be increased.

The values of BSF and SF obtained in this study have been compared with those reported by Russo et al in Table-2.

Accepted manuscript

ACCEPTED MANUSCRIPT

The obtained BSF values for various electron energies in reverse setup of the disk were also different. The BSF values for 6, 8, 10 and 12 MeV electron energy were equal to the 16.1%, 16.3%, 17.8% and 18.2%, respectively. The obtained PLD values were also equal to the 16.9% for 12 MeV, 16.2% for 10 MeV, 13.3% for 8 MeV, and 12.8% for 6 MeV in reverse position of shielding disk.

Fig. 6 shows the simulated 2D isodose distributions around the shielding disk for some incorrect configurations.

As shown in Fig. 6, the incorrect setups of shielding disk can considerably affect the dose uniformity inside the target area.

The S-index and V_{100} (a volume that receives 100% of dose) for all electron energies in different angles of the disk at correct and incorrect positions are compared in Table 3. These parameters were extracted from calculated differential-DVHs. The differential-DVHs for 12 MeV electron energy at different angles of disk position are shown in Fig. 7.

4. Discussion

Considering that a high single fraction of radiation dose is delivered during IOERT, it is very important to guarantee an accurate radiation dose has been delivered to the tumor area and underlying tissues are effectively spared.

Accepted manuscript

ACCEPTED MANUSCRIPT

Our results showed that by increasing the nominal energy of the electron beams, the SF of the disk slowly decreases. Simulation of the disk in incorrect setups with different angles (5°, 10°, 15°, 20°, 30°) showed that by increasing the angle of disk rotation, the SF decrements. Similarly, by increasing the angle of disk rotation, the PLD was also increased. The important issue in our result was that the BSF of the shielding disk at all studied positions and setups can affect the target dose distribution.

As it can be seen from Fig. 4, the BSF increases with the decrement of electron energy. In addition, by increasing the angle of disk rotation, BSF is also increased which can be due to the reduction of the distance between disk edge and of water phantom surface. Evaluation of incorrect disk setups showed that the maximum BSF and PLD occur at a part of the disk which is nearer to the surface. This leakage may be due to the bremsstrahlung production that increases in this region.

As shown from Fig. 7, the V_{100} decreases when the disk rotation angle is increased relative to the beam axis. Furthermore, the S-index increments by increasing the angle of disk rotation. Therefore, the disk rotation can influence the dose uniformity inside the target volume and would be improved with reduction of disk rotation angle. The study of Russo et al. shows the effect of disk rotation on the dose distribution in the target. Although they do not report

Accepted manuscript

ACCEPTED MANUSCRIPT

the homogeneity index, they show the reduction of target dose by increasing the disk rotation using cumulative-DVHs.

The proper setup of shielding disk and applicator is an important issue in IOERT procedure of breast cancer regarding both treatment and protection considerations. So far, there has been only one study about evaluating the dose distribution in IOERT procedures using GEANT4 MC code. In this study, Russo et al. have evaluated the BSF, SF, PLD and cumulative-DVH for the tumor bed in presence of a double layer disk consisted of 4 mm Aluminum and 2 mm lead for NOVAC7 accelerator (Russo et al. 2012). Although our work was similar to that of Russo et al in some aspects; but in the current study, a shielding disk composed of 3 mm PMMA and 3 mm steel was considered for electron beam produced by LIAC (12 MeV model) accelerator.

The reported BSFs and SFs by Russo et al were compared with those obtained in the current study (given in Table 2). As it can be seen from Table 2, in both studies, the BSF increases with a decrement of electron energy. The obtained BSFs in our study (at similar energies of 6, 8 and 10 MeV) were different from results of Russo et al. The maximum difference between the results of BSF was about 7.2%.

The SF variations with increasing the electron energy were in accordance with those reported by Russo et al. the maximum difference between our SF results and those of Russo study was about 4%.

Accepted manuscript

The difference between our results and those reported by Russo et al can be mainly attributed to the different employed IORT accelerator and shielding disk. Different accelerating structure of NOVAC 7 (employed by Russo et al) relative to the LIAC 12 MeV model (employed in our study) can considerably affect the energy characteristics of the electron beam from these two machines (Righi et al. 2013). This difference in electron energy spectrum can influence the BSF and SF parameters. In addition, the different material of employed disk in our study respect to the Russo's study, can also affect the electron interactions inside the shielding disk and, as a consequence, change the BSF and SF parameters.

One of the basic limitations in this study was the size of considered voxels for dose scoring. By increasing the voxel size, although the dose uncertainty is decreased, calculation of BSF, SF, and PLD in their real positions are not exactly possible due to the large size of scoring voxels. So, some over or under-estimation can occur in the calculation of these factors. Therefore, the size of scoring voxels should be chosen in such a way that there is a trade-off between dose uncertainty and precision of calculated parameters. Furthermore, when the disk is simulated in a rotated state, it may place inside some portion of scoring voxel which can affect the isodose distribution. This effect can be decreased by decrement of voxel size but at the expense of increased dose uncertainty.

Accepted manuscript

ACCEPTED MANUSCRIPT

Although the ionometric dosimetry was considered for validation of obtained MC results, it is also possible to substitute this dosimetry method by other ones such as gel dosimetry, provided that the uncertainty of measured dose has the acceptable range.

5. Conclusion

In this study, the effect of positional uncertainties related to shielding disk on target dose uncertainty and normal tissue over irradiation has been quantitatively evaluated through MC simulation. The results showed that introduced uncertainties can change the dosimetric characteristics inside the target volume and also lead to overexposure of underlying healthy tissue. Therefore, having an accurate information about disk position by C-arm imaging immediately before irradiation can help the treatment team to make more accurate decision concerning both disk setup and dose delivery to the target. As a result, treatment quality can be improved regarding both dose uncertainty inside the target volume and normal tissue complication probability.

Accepted manuscript

ACCEPTED MANUSCRIPT

References

Baghani, H. R., Aghamiri, S. M. R., Mahdavi, S. R., et al. (2015). "Comparing the dosimetric characteristics of the electron beam from dedicated intraoperative and conventional radiotherapy accelerators." J. Appl. Clin. Med. Phys. 16(2): 62-72.

Baghani, H. R., Aghamiri, S. M. R., Mahdavi, S. R., et al. (2015). "Dosimetric evaluation of Gafchromic EBT2 film for breast intraoperative electron radiotherapy verification." Phys. Med. 31(1): 37-42.

Catalano, M., Agosteo, S., Moretti, R., et al. (2007). "Monte Carlo simulation code in optimisation of the IntraOperative Radiation Therapy treatment with mobile dedicated accelerator." J. Phys. Conf. Ser. 74(1): 021002.

Ciocca, M., Cantone, M.-C., Veronese, I., et al. (2012). "Application of failure mode and effects analysis to intraoperative radiation therapy using mobile electron linear accelerators." Int. J. Radiat. Oncol. Biol. Phys. 82(2): e305-e311.

Gunderson, L. L., Willett, C. G., Calvo, F. A., et al. (2011). Intraoperative Irradiation: Techniques and Results, Humana Press.

Heidarloo, N., Baghani, H. R., Aghamiri, S. M. R., et al. (2017). "Commissioning of beam shaper applicator for conformal intraoperative electron radiotherapy." Appl. Radiat. Isot. 123: 69-81.

Intra, M., Luini, A., Gatti, G., et al. (2006). "Surgical technique of intraoperative radiation therapy with electrons (ELIOT) in breast cancer: a lesson learned by over 1000 procedures." Surgery 140(3): 467-471.

Kawrakow, I. (2005). "egspp: the EGSnrc C++ class library." National Research Council of Canada Report PIRS 899.

Kawrakow, I., Mainegra-Hing, E., Tessier, F., et al. (2009). "The EGSnrc C++ class library, NRC Report PIRS-898 (rev A)." National Research Council of Canada, Ottawa, Canada.

López-Tarjuelo, J., Bouché-Babiloni, A., Santos-Serra, A., et al. (2014). "Failure mode and effect analysis oriented to risk-reduction interventions in intraoperative electron radiation therapy: The specific impact of patient transportation, automation, and treatment planning availability." Radiother. Oncol. 113(2): 283-289.

Low, D. A. and Dempsey, J. F. (2003). "Evaluation of the gamma dose distribution comparison method." Med. Phys. 30(9): 2455-2464.

Low, D. A., Harms, W. B., Mutic, S., et al. (1998). "A technique for the quantitative evaluation of dose distributions." Med. Phys. 25(5): 656-661.

Ma, C., Reckwerdt, P., Holmes, M., et al. 0, Geiser B, and Walters B,(1995) DOSXYZ Users Manual, NRCC Report No, PIRS-0509B.

Accepted manuscript

ACCEPTED MANUSCRIPT

Martignano, A., Menegotti, L. and Valentini, A. (2007). "Monte Carlo investigation of breast intraoperative radiation therapy with metal attenuator plates." Med. Phys. 34(12): 4578-4584.

Oshima, T., Aoyama, Y., Shimozato, T., et al. (2009). "An experimental attenuation plate to improve the dose distribution in intraoperative electron beam radiotherapy for breast cancer." Phys. Med. Biol. 54(11): 3491.

Righi, S., Karaj, E., Felici, G., et al. (2013). "Dosimetric characteristics of electron beams produced by two mobile accelerators, Novac7 and Liac, for intraoperative radiation therapy through Monte Carlo simulation." J. Appl. Clin. Med. Phys. 14(1): 6-18.

Robatjazi, M., Mahdavi, S. R., Takavr, A., et al. (2015). "Application of Gafchromic EBT2 film for intraoperative radiation therapy quality assurance." Phys. Med. 31(3): 314-319.

Robatjazi, M., Tanha, K., Mahdavi, S., et al. (2016). "Monte Carlo Simulation of Electron Beams produced by LIAC Intraoperative Radiation Therapy Accelerator." J. biomed. phys. eng., http://dx.doi.org/10.22086/jbpe.v0i0.537.

Rogers, D., Kawrakow, I., Seuntjens, J., et al. (2003). "NRC user codes for EGSnrc." NRCC Report PIRS-702 (Rev. B).

Rogers, D., Ma, C., Walters, B., et al. (2002). "BEAMnrc Users Manual National Research Council of Canada." NRCC Report PIRS-0509 (A) revK.

Russo, G., Casarino, C., Arnetta, G., et al. (2012). "Dose distribution changes with shielding disc misalignments and wrong orientations in breast IOERT: a Monte Carlo–GEANT4 and experimental study." J. Appl. Clin. Med. Phys. 13(5): 74-92.

Severgnini, M., de Denaro, M., Bortul, M., et al. (2014). "In vivo dosimetry and shielding disk alignment verification by EBT3 GAFCHROMIC film in breast IOERT treatment." J. Appl. Clin. Med. Phys. 16(1): 112-120.

Yekta, Z. R., Mahdavi, S. R., Baghani, H. R., et al. (2016). "In vivo dosimetry using radiochromic films (EBT-2) during intraoperative radiotherapy." J Radiother Pract: 378-384.

Yoon, M. (2007). "A new homogeneity index based on the statistical analysis of dose volume histogram." J. Appl. Clin. Med. Phys. 8(2): 9-17.

Accepted manuscript

ACCEPTED MANUSCRIPT

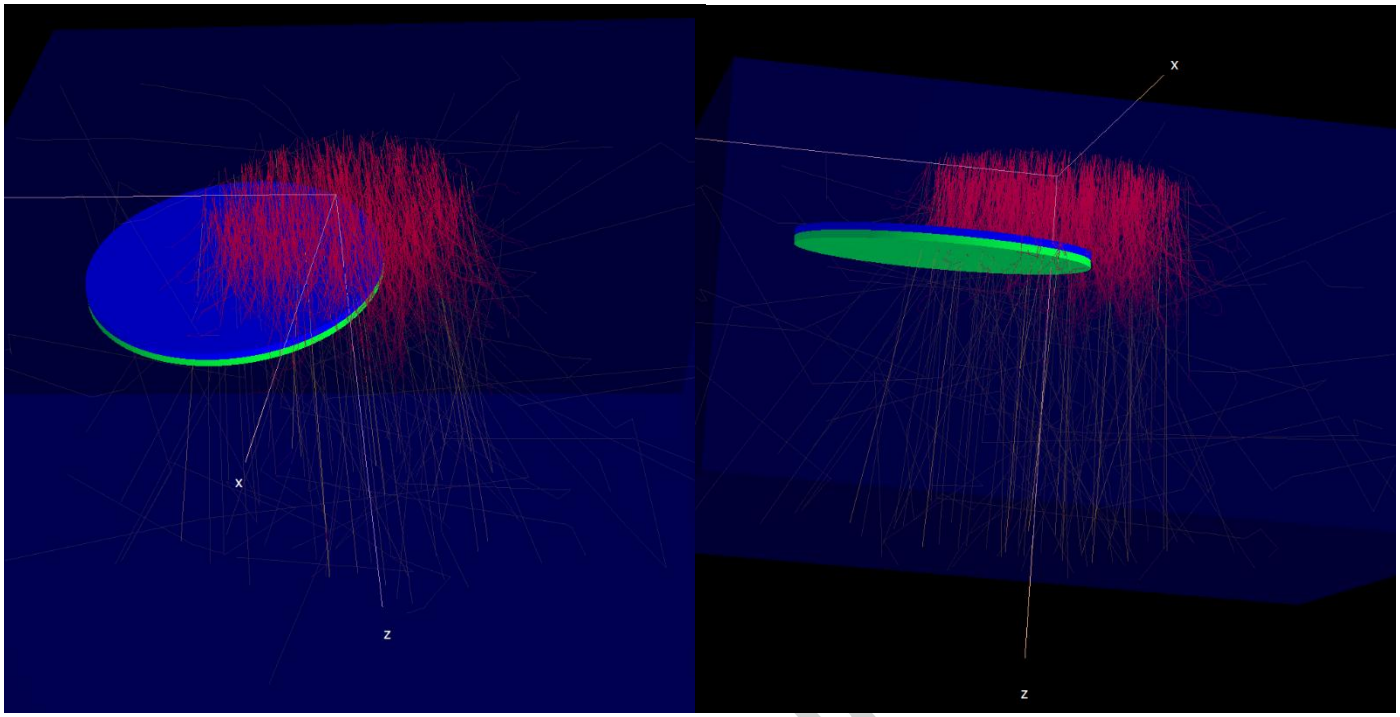

Figure *1*: Simulated shielding disk in the water phantom in incorrect configurations and beam tracking using EGS C++ user code. The images and tracks were obtained using EGS-view

Accepted manu

ACCEPTED MANUSCRIPT

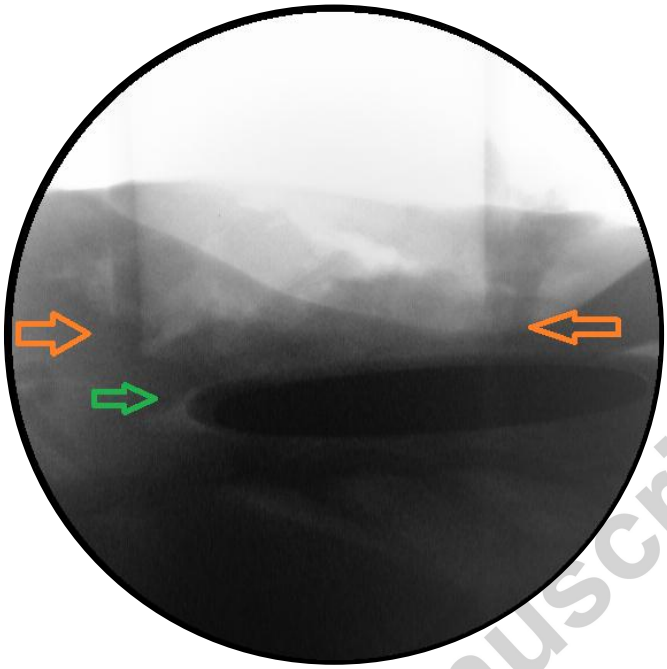

Figure *2*: C-arm images for verification of disk setup relative to the applicator obtained during breast IOERT. The disk and applicator size were equal to 80 mm and 70 mm, respectively. The orange arrows indicate the applicator end; the green arrow indicates the disk in an incorrect setup which is shifted about 15 mm from applicator edge.

Accepted manuscript

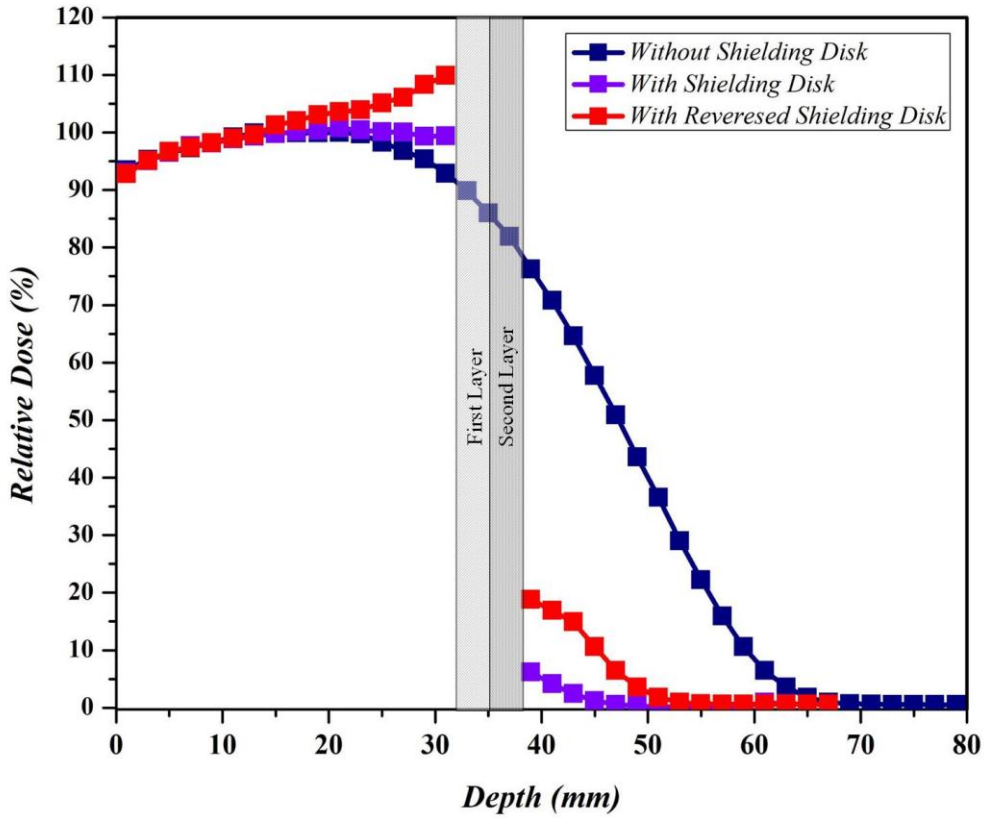

Figure 3: Simulated PDDs for 100 mm reference applicator at 12 MeV electron energy in presence and absence of shielding disk. The disk (120 mm diameter) was considered in both correct and reversed states at the depth of R90. When disk is in the correct state the first layer was considered as the low-Z material (PTFE) and in the incorrect state is considered as the high-Z material (STEEL)

Accepted m

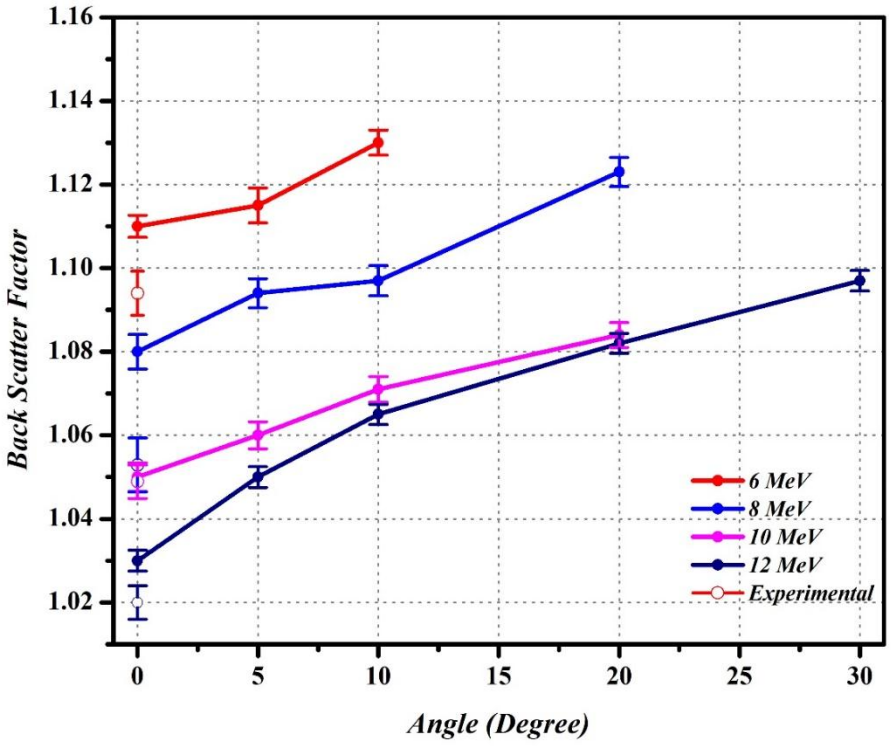

Figure 4: Simulated and experimental maximum BSF values at R90 depth of all energies for 100 mm diameter reference applicator and 120 mm diameter shielding disk in correct and incorrect setups of disk.

Accepted manuscript

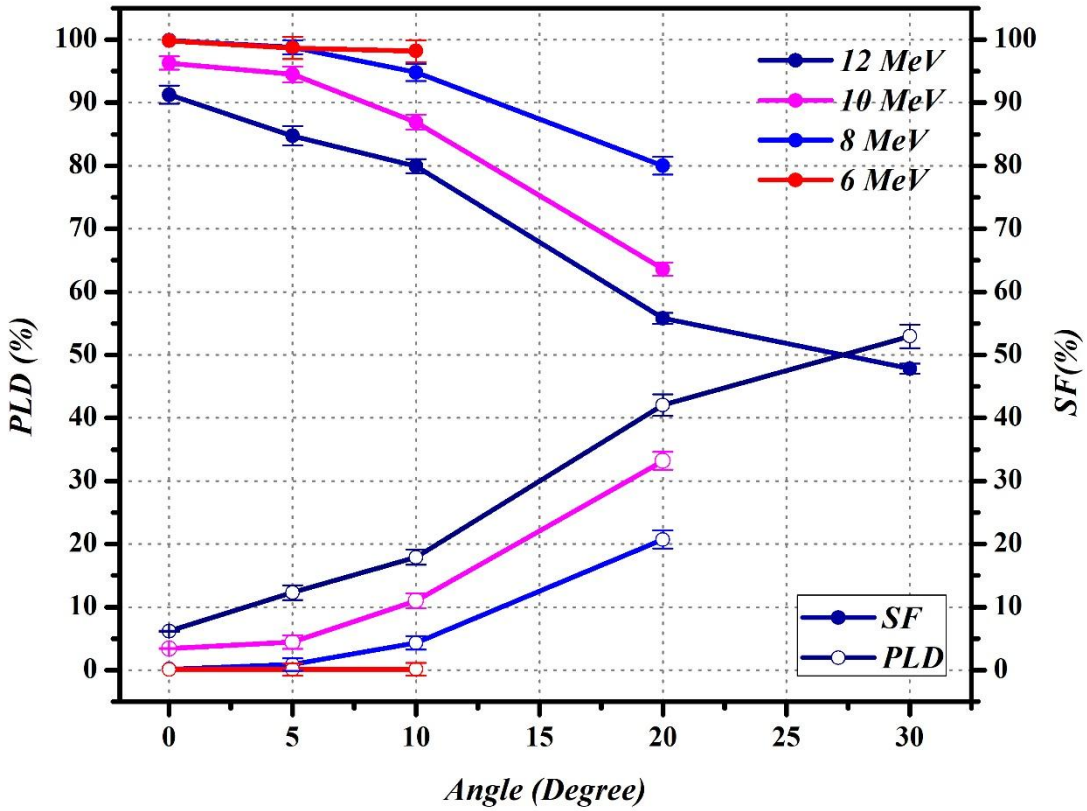

Figure 5: Maximum shielding factor and percentage of leakage for correct and incorrect setups of 120 mm diameter shielding disk. The disk was positioned at R90 of all nominal beam energies of the LIAC and irradiated by 100 mm reference applicator.

Accepted manuscript

ACCEPTED MANUSCRIPT

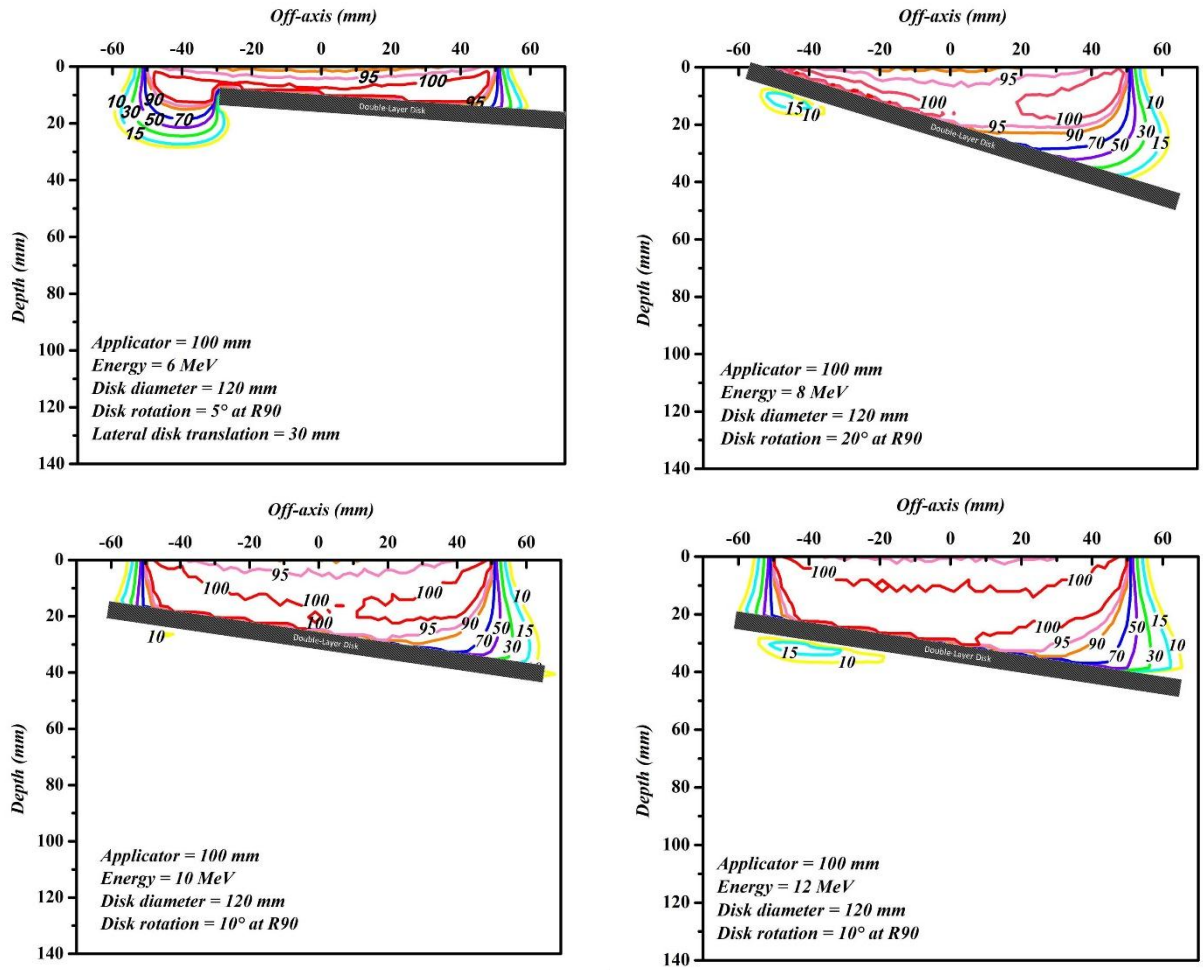

Figure 6: Simulated dose distributions in X-Z plane for incorrect setups of shielding disk at R90 depth of different energies.

Accepted m.

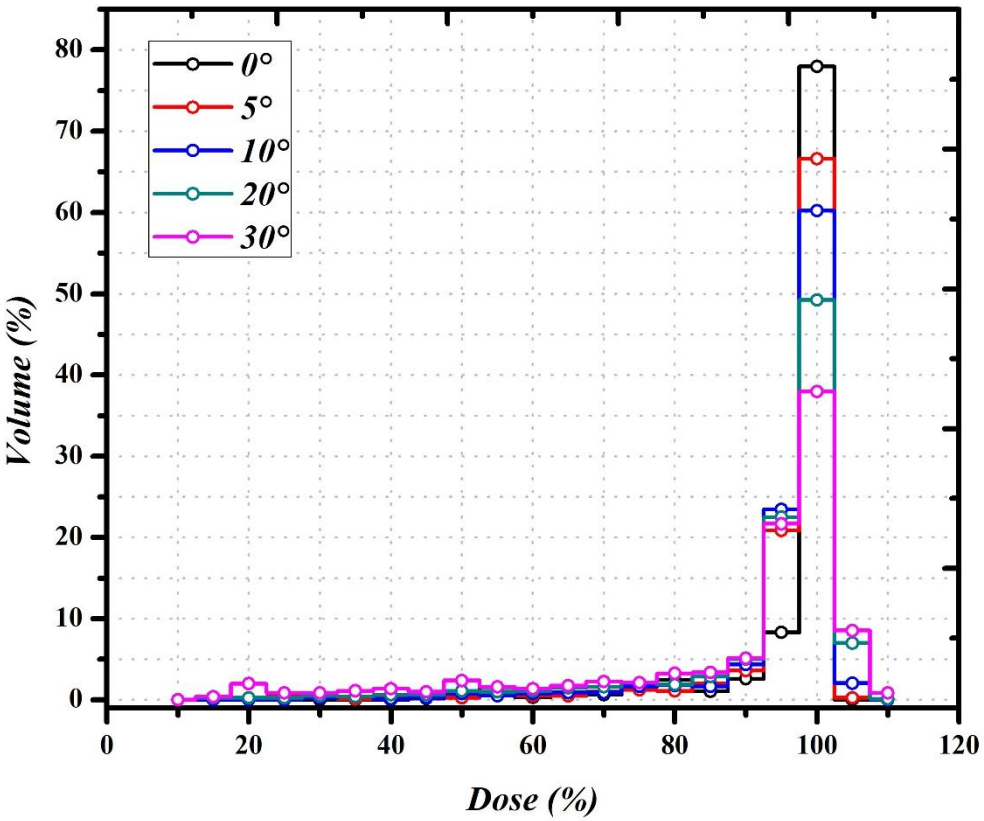

Figure 7: Differential-DVHs that obtained from simulation of 100 mm reference applicator and shielding disk with 120 mm diameter in correct and incorrect setups for 12 MeV beam energy. Considerable change is seen in V_{100}, when the shielding disk rotated relative to the applicator.

Accepted manuscript

ACCEPTED MANUSCRIPT

Table 1: Experimental and Monte Carlo calculated PDD parameters for 10 cm reference applicator of the LIAC.

Energy (MeV)	MC Calculations				Adv-Markus Chamber			
	R_{100} (mm)	R_{90} (mm)	R_P (mm)	R_{50} (mm)	R_{100} (mm)	R_{90} (mm)	R_P (mm)	R_{50} (mm)
6	8.8	14.8	29.1	21.8	8.2	14.1	28.6	21.3
8	12.2	21.5	41.8	31.6	12.1	21.9	41.6	31.6
10	16.6	28.2	51.7	40	15.7	27.3	52.2	40.0
12	16.5	31.9	61.2	47.1	16	31.6	61.2	46.7

Table-2: Comparison of BSF and SFs of current and Russo et al studies

Energy (MeV)	Current study		Russo et al study		BSFs relative difference (%)	SFs relative difference (%)
	BSF	SF (%)	BSF	SF (%)		
4	-	-	1.04		-	-
6	1.11	100	1.03	97.5	7.2	3
8	1.08	100	1.01	96.5	6.5	4
10	1.05	96	1.00	96.0	4.8	0
12	1.03	91	-	-	-	-

Accepted manuscript

ACCEPTED MANUSCRIPT

Table 3: Comparison of dose uniformity in correct and incorrect setup of the shielding disk using the S-index and V_{100}. An increase of disk rotation causes a decrease of V_{100} and an increase of the S-index.

Nominal E(MeV)	**Rotation of disk (°)**	**0**	**5**	**10**	**20**	**30**
6	V_{100} (%)	40.90	38.10	33.80	-	-
	SI	11.52	15.85	20.45	-	-
8	V_{100}	44.80	45.30	40.90	44.10	-
	SI	10.02	15.23	16.46	17.13	-
10	V_{100}	60.30	56.00	50.30	44.10	-
	SI	11.77	12.98	13.80	15.97	-
12	V_{100}	76.00	66.60	60.20	49.30	38.00
	SI	9.50	10.40	10.45	14.77	20.93

Accepted manuscript

ACCEPTED MANUSCRIPT

Highlights:

- A two-layer format of shielding disks is used in IOERT for protection of tissues.
- Dosimetric parameters of shielding disk were calculated with Monte Carlo simulation.
- Setup variation of shielding disk can affect the in-vivo dose distribution in IOERT.
- The dose distribution in various setups of the disk was demonstrated, quantitatively.

Accepted manuscript